Multichannel quantum-defect-theory analysis of the observed odd-parity 5*dnd* autoionization Rydberg series of neutral europium

S. Bhattacharyya, S. G. Nakhate, T. Jayasekharan, and M. A. N. Razvi*
Spectroscopy Division, Bhabha Atomic Research Centre, Mumbai 400085, India
(Received 13 April 2006; published 13 June 2006)

The spectra of autoionizing Rydberg series of europium atoms are analyzed by a semiempirical multichannel quantum defect theory (MQDT). Experimental data were obtained using two-step resonance ionization spectroscopy below the $5d\,^9D_J$ ionic multiplet. The MQDT model involving five channels and three limits is used to analyze the observed four odd-parity Rydberg series. Theoretical energies are computed and compared with the experimental values. The Rydberg series are assigned on the basis of calculated admixture coefficients. The series having $J=3/2$ are interpreted as 5*dnd* (2,3/2), 5*dnd* (2,5/2), 5*dnd* (3,3/2), and 5*dnd* (3,5/2). Interseries perturbations and perturbations due to levels of configuration 5*dnd* (4,5/2) are investigated. Some of the unobserved levels are also predicted.

DOI: 10.1103/PhysRevA.73.062506 PACS number(s): 32.30−r, 32.80.Rm, 32.80.Dz, 31.15.Ct

I. INTRODUCTION

The aim of this paper is to present multichannel quantum defect theory (MQDT) analysis of the autoionization Rydberg levels of neutral europium atoms below the ^9D threshold. MQDT has become one of the most successful theoretical methods for interpreting perturbed Rydberg and autoionization series. The theory was first derived by Seaton [1] and later extended in graphical form by Lu and Fano [2]. The theory was applied successfully in systems with closed shell configurations and systems with two valence electrons such as alkaline earth metals {Ca [3], Sr [4], Ba [5]} and Pb [6]. However, no report is found in the literature on MQDT analysis of lanthanide atoms except for Yb [7], which again has a closed 4*f* shell ground-state configuration. The ground-state configuration of europium atoms is $4f^7\,6s^2$ and the spectrum of europium is more complex due to its half filled 4*f* shell.

Experimentally, there are only few studies on bound and autoionization Rydberg series of europium {Smith and Tomkins [8] and Zyuzikov *et al.* [9]}. In the earlier works from our laboratory, we have extensively studied odd-parity bound and autoionization Rydberg series converging to the $^9S_4$ and $^7S_3$ limits, respectively [10,11]. The spectra were, however, not interpreted using MQDT. Complexity in MQDT analysis increases due to the fact that even the lower levels of configurations such as $4f^7\,6p^2$, $4f^7\,5dns$, $4f^7\,5dnd$, and $4f^6nln'1'n''1''$ and their corresponding terms are not identified. Here we report four odd-parity autoionization Rydberg series of $J=3/2$ converging to the $5d\,^9D_J$ ionic multiplet levels and attempt interpretation of the spectrum by multichannel quantum defect theory.

II. EXPERIMENTAL DETAILS

The details of the experimental setup were described in our earlier publication [12]. In brief, vapor of neutral europium was generated in a heat-pipe oven by heating europium metal to 800 K. Two tunable dye lasers with typical linewidth of 0.2 cm^{-1}, pumped by a XeCl excimer laser were used in this study. Pulse energy of the dye lasers was about 0.5 mJ and beam diameter was 5 mm in the interaction region. The excitation scheme for approaching autoionization resonances in the spectra of Eu I is shown in Fig. 1. The atoms were excited to the intermediate states of configuration $4f^7\,5d6p\,^8P_{5/2,7/2}$ at energy values 28 667.39 and 28 918.17 cm^{-1} using *p*-terphenyl dye in the first dye laser. The second dye laser, pumped by the same excimer laser,

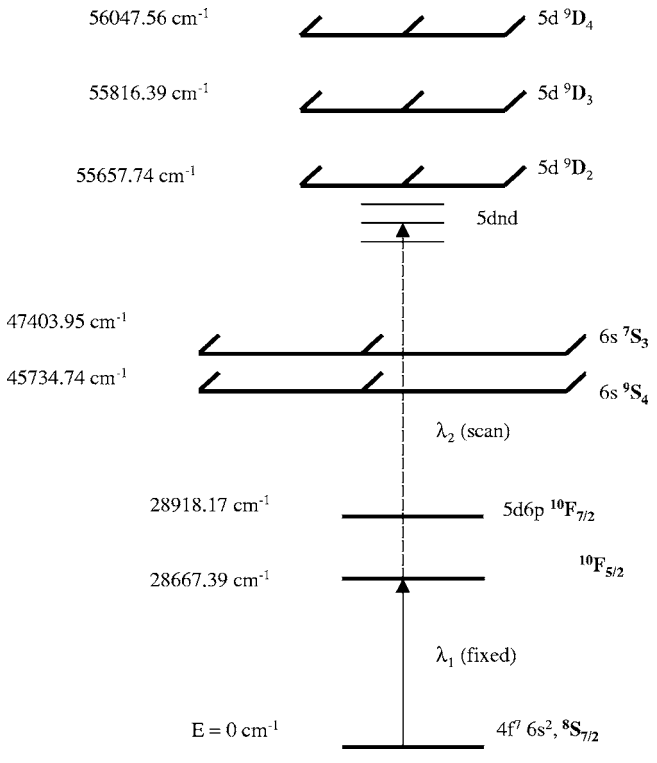

FIG. 1. Schematic diagram of the two-step laser excitation scheme for studying odd-parity 5*dnd* autoionization resonances in the spectra of europium atom.

*Corresponding author. Email address: mrazvi@barc.gov.in

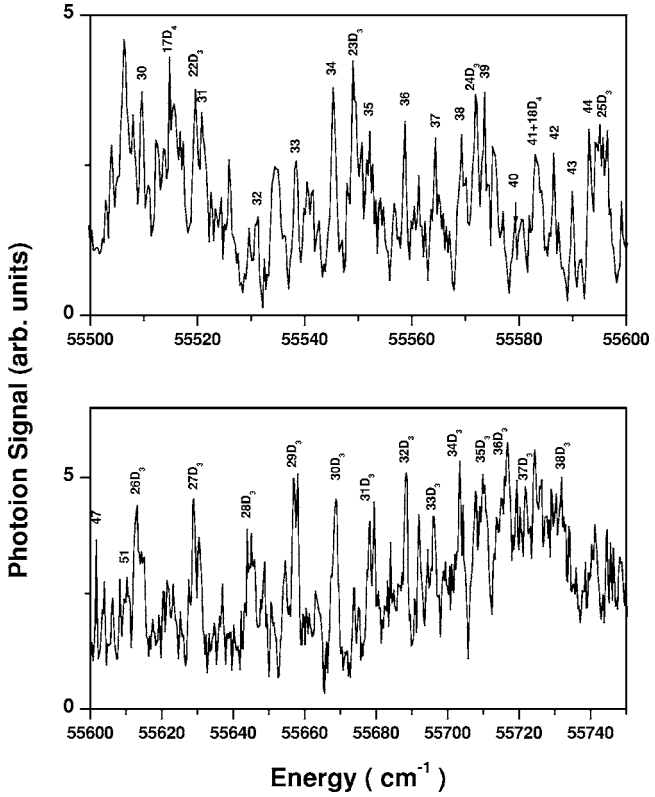

FIG. 2. A portion of the observed two-color photoionization spectrum of europium atom. Integer n represents principal quantum number of series converging to $5d\,^9D_2$ limit, nD_3 and nD_4 represent n values of members of the series converging to the $5d\,^9D_3$ and $5d\,^9D_4$ limit, respectively.

was scanned to probe the energy region 54 920–55 817 cm^{-1} by using Butyl-PBD dye. The laser pulse from the second dye laser reaches the interaction zone with a delay of 12 ns with respect to the first dye laser pulse. Care was taken to have optimum spatial and temporal overlap of these two dye laser pulses. Photoions produced in the two-step laser photoionization process were detected by an externally heated hot cathode thermionic diode mounted inside the heat pipe. The photoionization signal was processed by a boxcar averager and recorded as a function of the wavelength of the scanning laser on a personal computer. The signal from a uranium-neon hollow cathode discharge lamp and the transmission fringes of the Fabry-Perot etalon were simultaneously recorded by the two independent channels of a boxcar averager for calibration of the wavelength of the scanning laser. The level energies were determined using a subroutine based on interpolation that takes into account uranium reference lines and interference fringes and yields energies of all unknown resonances. A part of the photoionization signal in the energy range 55 500–55 750 cm^{-1} is shown in Fig. 2.

III. RESULTS AND DISCUSSIONS

The experimental energies are deduced from the energy-level positions of the spectral lines, which are quite symmetric and narrow. The width of most of the autoionization resonances is of the order of 1 cm^{-1} or less. The uncertainty of our measurements is estimated to be $\approx$0.5 cm^{-1} limited mainly by the linewidth of the laser and data acquisition speed. The total angular momentum quantum number J was assigned to all the observed energy levels using single photon selection rules ($\Delta J=0, \pm 1$ but $0 \leftrightarrow 0$ forbidden) and by comparing the photoionization spectra obtained by employing intermediate levels with different J. The levels are then grouped as per their J-quantum number. The effective principal quantum number ν is obtained from the Rydberg-Ritz formula as $\nu=\sqrt{R/I_i-E}$, where R is the mass corrected Rydberg constant for Eu I ($R=109\,736.918$ cm^{-1}), E is the observed level energy and I_i is the energy of the ionic level to which the series is converging. The different Rydberg series are constructed by observing the monotonic variation of $1-\nu$ (mod 1) with energy, spectral line shape, and intensity of the resonance. The assignment of the series members is confirmed by MQDT analysis.

The excitation scheme for accessing the autoionization resonances is shown in Fig. 1. The accessible series with $J=3/2$ from intermediate levels $4f^7\,5d6p\,^8P$ in jj coupling are the following:

$$5d6p\,^8P \rightarrow 5dnd(2,j) \text{ with } j=3/2 \text{ and } 5/2,$$

$$\rightarrow 5dnd(3,j) \text{ with } j=3/2 \text{ and } 5/2,$$

$$\rightarrow 5dnd(4,5/2),$$

$$\rightarrow 5dns(2,3/2).$$

We have observed four series, two converging to the $^9D_2$ and the other two to the $^9D_3$ limit. The values for ν (mod 1) for the observed series members converging to the $5d\,^9D_2$ and $5d\,^9D_3$ limit are in the range of 0.2–0.35. Two levels of $4f^7\,5d(^9D)\,6s$ and $4f^7\,5d^2$ configurations are listed in the NBS table [13]. The ν value is 1.60 for $5d\,(^9D)\,6s$ and 2.30 for $5d^2$ level, calculated with respect to the fine structure average of $5d\,^9D_J$ limit. Hence we conclude the observed series have $5d\,(^9D)\,nd$ configuration and this has been confirmed by the MQDT analysis presented in later sections. We could observe the two $5dnd\,(2,j)$ with $j=3/2$ and $5/2$ series distinctly from $n=15$ to 26. From $n=27$ onwards, we could not resolve the members of these series but these two series are observed unresolved up to $n=51$. The two $5dnd$ series converging to the $5d\,^9D_3$ ionic level are observed from $n=14-24$. The members of these two series are observed up to $n=53$, but we could not resolve them beyond $n=24$. We have not observed the Rydberg series of configuration $5dns\,(2,3/2)$ expected to converge to $5d\,^9D_2$ ionic level. Five levels of $5dnd\,(4,5/2)$ configuration are identified in the spectrum. The experimental energies, theoretically calculated energy values, admixture coefficients and their assignment are given in Table I. In Fig. 2, we have shown the unresolved members of $5dnd\,(2,j)$ with $j=3/2, 5/2$ series from $n=30$ to 51. The members of $5dnd$ series converging to the $5d\,^9D_3$ limit are marked as nD_3 in the spectrum and is shown from $n=22$ to 38. Two levels of $5dnd\,(4,5/2)$ configuration are shown in the spectrum for $n=17$ and 18 and is marked as

TABLE I. Experimental, theoretical energies and their assignments of $J=3/2$ autoionization series below $5d\,^9D$ threshold. Admixture coefficients larger than 10% in a channel are given in brackets. The experimentally unresolved members of the two series of a given n converging to $^9D_2$ and $^9D_3$ limits are listed as $5dnd(2,\ j)$ and $5dnd(3,\ j)$, respectively. Channels $5d(^9D_2)nd_{5/2}$, $5d(^9D_2)nd_{3/2}$, $5d(^9D_3)nd_{5/2}$, $5d(^9D_3)nd_{3/2}$, and $5d(^9D_4)nd_{5/2}$ are represented as 1, 2, 3, 4, and 5, respectively.

Assignment	E_{EXPT} (cm^{-1})	E_{TH} (cm^{-1})	E_{EXPT}-E_{TH}	Admixture coefficients in other channels
5*d* 15*d* (2,3/2) [62]	54923.3	54924.7	−1.4	4 [24], 1 [14]
5*d* 15*d* (2,5/2) [80]	54930.3	54931.7	−1.4	
5*d* 14*d* (3,3/2) [5]	54948.8	54948.6	0.2	1 [66], 3 [28]
5*d* 14*d* (3,5/2) [89]	54961.6	54962.2	−0.6	
5*d* 13*d* (4,5/2) [40]		55024.3		1 [54]
5*d* 16*d* (2,3/2) [67]	55035.2	55034.7	0.5	1 [29]
5*d* 16*d* (2,5/2) [64]	55046.3	55045.8	0.6	5 [26]
5*d* 15*d* (3,3/2) [95]	55082.1	55081.0	1.1	
5*d* 15*d* (3,5/2) [95]	55095.6	55093.6	2.0	
5*d* 17*d* (2,5/2) [65]	55117.7	55118.6	−0.9	2 [31]
5*d* 17*d* (2,3/2) [42]		55124.2		1 [50]
5*d* 16*d* (3,3/2) [53]	55182.8	55182.3	0.5	2 [42]
5*d* 18*d* (2,5/2) [50]	55186.2	55186.1	0.1	2 [22], 4 [12]
5*d* 18*d* (2,3/2) [55]	55190.3	55191.4	−1.1	4 [21], 5 [15]
5*d* 16*d* (3,5/2) [89]	55199.1	55199.3	−0.2	
5*d* 14*d* (4,5/2) [59]	55205.7	55206.4	−0.7	4 [19], 1 [17]
5*d* 19*d* (2,3/2) [61]	55244.1	55243.3	0.8	1 [36]
5*d* 19*d* (2,5/2) [70]	55246.9	55246.4	0.5	2 [24]
5*d* 17*d* (3,3/2) [11]	55270.8	55272.7	−1.9	3 [45], 1 [34]
5*d* 17*d* (3,5/2) [93]	55280.3	55280.9	−0.6	
5*d* 20*d* (2,5/2) [70]	55289.8	55289.7	0.1	2 [23]
5*d* 20*d* (2,3/2) [45]		55293.0		1 [44]
5*d* 21*d* (2,5/2) [56]	55328.0	55327.6	0.4	2 [22], 5 [13]
5*d* 21*d* (2,3/2) [72]	55329.5	55328.7	0.8	1 [21]
5*d* 15*d* (4,5/2) [29]	55338.0	55336.0	2.0	1 [51], 4 [19]
5*d* 18*d* (3,3/2) [82]	55344.4	55344.3	0.1	
5*d* 18*d* (3,5/2) [95]	55348.5	55349.0	−0.5	
5*d* 22*d* (2,3/2) [44]	55363.3	55362.5	0.8	1 [53]
5*d* 22*d* (2,5/2) [59]		55364.7		2 [34]
5*d* 23*d* (2,3/2) [70]	55390.3	55390.3	0.0	1 [22]
5*d* 23*d* (2,5/2) [75]	55392.1	55391.7	0.4	2 [19]
5*d* 19*d* (3,3/2) [13]	55399.6	55399.4	0.2	1 [45], 3 [33]
5*d* 19*d* (3,5/2) [94]	55404.8	55404.5	0.3	
5*d* 24*d* (2,5/2) [81]	55415.3	55414.8	0.5	2 [16]
5*d* 24*d* (2,3/2) [51]	55417.3	55416.5	0.8	1 [43]
5*d* 16*d* (4,5/2) [53]	55435.5	55434.0	1.5	1 [36]
5*d* 25*d* (2,3/2) [58]	55436.0	55436.3	−0.3	5 [21], 4 [16]
5*d* 25*d* (2,5/2) [72]	55438.8	55439.6	−0.8	5 [19]
5*d* 20*d* (3,3/2) [89]	55445.3	55446.8	−1.5	
5*d* 20*d* (3,5/2) [95]	55450.1	55450.5	−0.4	
5*d* 26*d* (2,5/2) [60]	55455.2	55455.2	0.0	2 [36]
5*d* 26*d* (2,3/2) [34]	55456.3	55456.8	−0.5	1 [56]
5*d* 27*d* (2,*j*)	55471.2	55471.9	−0.7	1+2 [98]
5*d* 21*d* (3,3/2) [40]	55485.4	55484.3	1.1	1+2 [57]
5*d* 28*d* (2,*j*)	55486.4	55486.8	−0.4	1+2 [86], 3 [12]

TABLE I. (*Continued.*)

Assignment	E_{EXPT} (cm^{-1})	E_{TH} (cm^{-1})	E_{EXPT}-E_{TH}	Admixture coefficients in other channels
5*d* 21*d* (3,5/2) [86]	55489.4	55489.8	−0.4	1+2 [11]
5*d* 29*d* (2,*j*)	55498.2	55499.0	−0.8	1+2 [98]
5*d* 30*d* (2,*j*)	55509.2	55510.2	−1.0	1+2 [97]
5*d* 17*d* (4,5/2) [28]	55514.5	55517.1	−2.6	4 [63]
5*d* 22*d* (3,3/2) [60]	55519.3	55519.0	0.3	1+2 [38]
5*d* 31*d* (2,*j*)	55520.4	55520.6	−0.2	1+2 [90]
5*d* 22*d* (3,5/2) [95]	55522.3	55522.3	0.0	
5*d* 32*d* (2,*j*)	55530.8	55530.1	0.7	1+2 [98]
5*d* 33*d* (2,*j*)	55538.3	55538.3	0.0	1+2 [98]
5*d* 34*d* (2,*j*)	55545.4	55545.5	−0.1	1+2 [89]
5*d* 23*d* (3,3/2) [38]	55548.8	55548.2	0.6	1+2 [52]
5*d* 23*d* (3,5/2) [88]	55550.0	55550.5	−0.5	1+2 [11]
5*d* 35*d* (2,*j*)	55552.3	55552.7	−0.4	1+2 [93]
5*d* 36*d* (2,*j*)	55558.3	55558.8	−0.5	1+2 [99]
5*d* 37*d* (2,*j*)	55563.8	55564.5	−0.7	1+2 [99]
5*d* 38*d* (2,*j*)	55568.9	55569.6	−0.7	1+2 [96]
5*d* 24*d* (3,3/2) [69]	55571.9	55572.4	−0.5	1+2 [23]
5*d* 39*d* (2,*j*)	55573.3	55574.4	−1.1	1+2 [76], 3 [22]
5*d* 24*d* (3,5/2) [71]	55574.9	55575.3	−0.4	1+2 [26]
5*d* 40*d* (2,*j*)	55578.7	55578.8	−0.1	1+2 [93]
5*d* 41*d* (2,*j*)	55583.1	55582.5	0.6	1+2 [86], 5 [11]
5*d* 18*d* (4,5/2) [52]	55583.4	55584.4	−1.0	1+2 [41]
5*d* 42*d* (2,*j*)	55586.5	55586.9	−0.4	1+2 [93]
5*d* 43*d* (2,*j*)	55590.4	55590.2	0.2	1+2 [96]
5*d* 44*d* (2,*j*)	55592.6	55593.3	−0.7	1+2 [96]
5*d* 25*d* (3,*j*)	55595.1	55595.3	−0.2	3+4 [77], 1+2 [21]
5*d* 45*d* (2,*j*)		55596.6	—	1+2 [81]
5*d* 46*d* (2,*j*)	55599.2	55599.3	−0.1	1+2 [99]
5*d* 47*d* (2,*j*)	55601.4	55601.8	−0.4	1+2 [100]
5*d* 48*d* (2,*j*)	55603.8	55604.3	−0.5	1+2 [100]
5*d* 49*d* (2,*j*)	55606.1	55606.5	−0.4	1+2 [100]
5*d* 50*d* (2,*j*)	55608.2	55608.6	−0.4	1+2 [100]
5*d* 51*d* (2,*j*)	55610.3	55610.6	−0.3	1+2 [100]
5*d* 26*d* (3,*j*)	55613.2	55614.2	−1.0	3+4 [63], 1+2 [33]
5*d* 27*d* (3,*j*)	55628.6			
5*d* 28*d* (3,*j*)	55643.5			
5*d* 29*d* (3,*j*)	55656.6			
5*d* 30*d* (3,*j*)	55668.2			
5*d* 31*d* (3,*j*)	55677.8			
5*d* 32*d* (3,*j*)	55688.4			
5*d* 33*d* (3,*j*)	55696.0			
5*d* 34*d* (3,*j*)	55703.3			
5*d* 35*d* (3,*j*)	55710.0			
5*d* 36*d* (3,*j*)	55716.4			
5*d* 37*d* (3,*j*)	55722.5			
5*d* 38*d* (3,*j*)	55729.6			
5*d* 39*d* (3,*j*)	55733.3			
5*d* 46*d* (3,*j*)	55757.6			

TABLE I. (*Continued.*)

Assignment	E_{EXPT} (cm^{-1})	E_{TH} (cm^{-1})	E_{EXPT}-E_{TH}	Admixture coefficients in other channels
$5d\ 47d\ (3,j)$	55760.2			
$5d\ 48d\ (3,j)$	55762.7			
$5d\ 49d\ (3,j)$	55764.7			
$5d\ 50d\ (3,j)$	55766.9			
$5d\ 51d\ (3,j)$	55769.0			
$5d\ 52d\ (3,j)$	55771.1			
$5d\ 53d\ (3,j)$	55772.6			

nD_4. A broad perturbation is observed in the spectrum centered at 55 726 cm^{-1}. It appears that the influence of this perturbing level spreads over a large number of members of $5dnd\ (3,j)$ series as clearly shown in Fig. 2. We could not identify members of this series from $n=40$ to 45 clearly due to presence of this perturber. The origin of this perturbing level is not known. This point will be discussed in more detail in Sec. IV C.

IV. THEORETICAL ANALYSIS

A. Basic formulas of MQDT

The detailed descriptions of basic ideas and formulas of MQDT have been presented in many works, as mentioned in the Introduction. We only summarize the basic formulas of MQDT here.

MQDT relies on the basic idea that when the distance of an excited electron, r is greater than distance r_o of the ion core, it moves in a Coulomb potential. For $r \geqslant r_o$, the wave function of the electrons is constructed by the superposition of the "collision channels" wave function. The collision channels are characterized by the state of the ion core, the state of the valence electron, and their coupling. In the non-Coulomb region, $r < r_o$, the wave function is considered to be the normal scattering modes, produced by the linear combinations of incoming Coulomb wave functions reflected from the ion core with only a phase shift. These normal modes are known as "close-coupling eigen channels" α, characterized by the eigenquantum defect μ_α and an orthogonal matrix $U_{i\alpha}$ which connects collision channels i with close-coupling channels α. These two bases collision channels and close-coupling channels are equated at $r=r_o$.

For the discrete spectrum, the boundary condition at $r=\infty$ leads to the following condition:

$$\sum_{\alpha=1}^{N} A_\alpha U_{i\alpha} \sin \pi(\nu_i + \mu_\alpha) = 0, \tag{1}$$

where the summation is over the number of channels, N.

For the nontrivial solution for A_α,

$$\det\left|U_{i\alpha} \sin \pi(\nu_i + \mu_\alpha)\right| = 0. \tag{2}$$

This equation describes a surface S in the N-dimensional space of ν_i.

Each observed energy level is assigned as many ν_i as there are relevant series limit $M(M \leqslant N)$ such that

$$E = I_i - \frac{R}{\nu_i^2}, \tag{3}$$

where $i=1,\ldots,M$.

In this work, three ionization limits involved are $I_1=55\,657.74\ cm^{-1}$, $I_2=55\,816.39\ cm^{-1}$, and $I_3=56\,047.56\ cm^{-1}$ and effective quantum numbers determined with respect to these limits are ν_1, ν_2, and ν_3, respectively.

Theoretical energy positions are determined by the intersections of surface S and curve L defined by Eq. (3). In graphical representation of MQDT, $1-\nu_j$ (mod 1) vs ν_i (mod 1) curves, known as Lu-Fano curves are constructed and MQDT parameters are determined by fitting theoretical energies to the experimental ones.

B. Autoionization spectra in the energy region 54 920 cm^{-1} to $5d\ ^9D_2$ limit

1. MQDT channels

All the autoionization resonances observed are symmetric and narrow. The open channels based on $6s$ continuum, $6s\varepsilon l$ are ignored as the resonances are sharp and their widths are smaller than the spacing between two successive series members. A similar situation arises for $3dnd$ autoionization series converging to the $3d_{j=3/2,5/2}$ limit in the case of the calcium atom [3]. The channel based on $5dns\ (2,1/2)$ configuration is also ignored, as $5dns$ channels are expected to have negligible coupling with $5dnd$ channels. In this energy region, our model includes five interacting closed channels and three ionic limits. We define the collision channels in jj coupling, and the close-coupling channels in LS coupling. The channels are shown in Table II.

2. MQDT parameters

The collision channels are described in jj coupling in order to take into account the spin-orbit coupling effect. Since the α eigenchannels are expected to be nearly LS coupled, an intermediate basis $\bar{\alpha}$ of exactly LS coupled channel is introduced by factorizing matrix elements $U_{i\alpha}$ in the form

TABLE II. MQDT parameters for odd-parity $J=3/2$ autoionization spectrum.

$i, \alpha, \bar{\alpha}$	1	2	3	4	5
$\|i\rangle$	$5d(^9D_2)nd_{5/2}$	$5d(^9D_2)nd_{3/2}$	$5d(^9D_3)nd_{5/2}$	$5d(^9D_3)nd_{3/2}$	$5d(^9D_4)nd_{5/2}$
I_i	55657.74	55657.74	55816.39	55816.39	56047.56
$\|\bar{\alpha}\rangle$	$5dnd\ ^{10}G_{3/2}$	$5dnd\ ^{8}G_{3/2}$	$5dnd\ ^{10}F_{3/2}$	$5dnd\ ^{8}F_{3/2}$	$5dnd\ ^{8}D_{3/2}$
μ_α^o	0.8235	0.7469	0.6861	0.6578	0.5547
μ_α^1	2.2104	1.9540	−0.1725	−1.6083	−2.1004
$U_{i\bar{\alpha}}$	−0.3412	0.7971	−0.1782	0.4383	0.1565
	0.7817	0.1782	0.4083	0.3652	0.2391
	−0.1009	−0.5406	−0.3689	0.5893	0.4629
	−0.4944	−0.1127	0.7746	0.0000	0.3780
	−0.1336	0.1675	−0.2559	−0.5122	0.7492
$V_{\bar{\alpha}\alpha}$	$\theta_{13}=-0.5445$	$\theta_{24}=0.3305$	$\theta_{15}=0.0792$	$\theta_{25}=-0.4319$	$\theta_{35}=-0.0184$
	$\theta_{45}=0.1362$				
$U_{i\alpha}$	−0.1865	0.7419	−0.3389	0.2257	0.4990
	0.4747	0.1761	0.7484	0.3280	0.2756
	0.1411	−0.4804	−0.3729	0.7628	0.1688
	−0.7917	−0.2818	0.3999	0.0857	0.3559
	0.0775	−0.3191	−0.3004	−0.4431	0.7352

$$U_{i\alpha} = \sum_{\bar{\alpha}} U_{i\bar{\alpha}} V_{\bar{\alpha}\alpha}. \tag{4}$$

The $U_{i\bar{\alpha}}$ matrix elements are exactly known from *LS-jj* transformation matrix [14]. The matrix elements $V_{\bar{\alpha}\alpha}$ are not directly fitted; instead the orthogonal matrix V is generated by successive rotations in the (jk) planes as

$$V = \prod_{q=1}^{N(N-1)/2} V_q(\theta_q), \tag{5}$$

where $V_q(\theta_q)$ for the combination $q=(j,k)$ is defined in Appendix B of Lee and Lu [15], N is the number of channels. These θ_{jk} angles are optimized and a good fit is obtained by factorizing V in the form

$$V = V_{13}(\theta_{13})V_{24}(\theta_{24})V_{15}(\theta_{15})V_{25}(\theta_{25})V_{35}(\theta_{35})V_{45}(\theta_{45}). \tag{6}$$

No energy dependence is considered for these angles.

For the eigenquantum defects μ_α, linear energy dependence is introduced as

$$\mu_\alpha = \mu_\alpha^o + \Delta E \mu_\alpha^1, \tag{7}$$

where $\Delta E = \frac{(I_3 - E)}{R}$.

3. Interpretation of the energy levels

The optimization of parameters μ_α^o's, μ_α^1's, and θ_{jk}'s are carried out by fitting theoretical energies to the experimental energies in the energy region 54 909.5–55 542.0 corresponding ν_2 from 11.0 to 20.0. This includes fitting of 48 experimentally observed levels with rms deviation 0.1 cm^{-1}. A projection of the three-dimensional Lu-Fano plot in the plane of (ν_1, ν_2) is shown in Fig. 3. The theoretical solid curves are obtained with the optimal set of parameters given in Table II. The Lu-Fano plot consists of quasihorizontal and quasivertical branches, signifying a relatively weak interaction between channels 1 and 2 with channels 3 and 4. The peculiarities and nonmonotonic behavior of the branches has to originate from $5dnd$ $(4,5/2)$ perturbers. Thus all the parameters connecting channel 5 with i channels (for $i=1$, 2, 3, and 4) $V_{i5}(\theta_{i5})$ were optimized. The theoretical energy values and the difference between theoretical and experimental energies are shown in Table I.

Using the MQDT parameters obtained by optimization in the energy region $\nu_2=11.0-20.0$, theoretical energies are calculated between $\nu_2=20.0$ ($E=55\,542.0$ cm^{-1}) to $5d\ ^9D_2$ series limit ($E=55\,657.74$ cm^{-1}). The agreement between theoretical and experimental energies is quite satisfactory. In most cases, the agreement is within an error of 1 cm^{-1} or less. The maximum discrepancy of 2.6 cm^{-1} is observed for the $5d17d$ $(4,\ 5/2)$, level. For the two $5dnd$ series converging the $5d\ ^9D_2$ series limit, we have not been able to resolve experimentally the two series members for $n=27$ onwards and we have listed them in the table as $5dnd$ $(2,j)$ with $j=3/2,\ 5/2$. Since the differences in theoretical energies for these levels are within 0.5 cm^{-1}, we have given the average values for their energies; and the sum of admixture coefficients for the pair of levels are listed in Table I. Similarly, from $n=25$ onwards, we have listed the observed energies as $5dnd$ $(3,j)$ with $j=3/2,\ 5/2$ in the table for the series converging to $5d\ ^9D_3$ limit, as we could not resolve them experimentally.

4. Wave functions

In addition to the theoretical energy-level positions, MQDT gives the wave functions of the Rydberg levels. The

expansion coefficient $Z_i^{(n)}$ of the ith collision channel in the nth eigenstate $\Psi^{(n)}$ is given as

$$Z_i^{(n)} = (-1)^{l_i+1} \nu_i^{3/2} \sum_\alpha A_\alpha^{(n)} \frac{1}{N_n} U_{i\alpha} \cos \pi(\nu_i^{(n)} + \mu_\alpha), \quad (8)$$

where N_n is a normalization factor [15]. We have calculated the admixture coefficients for all the levels based on the MQDT parameters given in Table II. Admixture coefficients of larger than 10% in a channel are listed in Table I. The series assignment is done based on admixture coefficients. We have assigned the series in jj coupling, as this is more direct, since the j value of the core electron is well defined [16].

It appears that all the perturbations in the spectrum are quite localized. A strong channel mixing is observed between the two series converging to the $^9D_2$ limit. The coupling between the two series converging to $^9D_3$ limit appears to be very weak. The $5dnd$ (4,5/2) configuration based levels mixes very strongly with the $5dnd$ (2,5/2) Rydberg series members and less strongly with $5dnd$ (3,5/2) configuration based levels. The coupling of $5dnd$ (4,5/2) levels to other channels is insignificant. An admixture coefficient of nearly ≈90% is observed for most of the levels converging to $^9D_3$ limit, signifying that these levels are well described in jj coupling. The admixture coefficient for the Rydberg series members converging to $^9D_2$ limit is in the range of 50–80 %.

C. Autoionization spectra in the energy region between $5d\,^9D_2$ to $5d\,^9D_3$ limit

In this energy range channel 1 and 2 becomes open channels, $5d\,(^9D_2)\,\varepsilon l$. But the observed autoionization resonances remain symmetric and narrow. This is because of the weak coupling between these levels with channel 1 and 2. But a broad perturbation is observed in the spectrum centered at energy ~55 726 cm^{-1}. It is apparent in the spectrum, as shown in Fig. 2, that the effect of this perturbation is observed on $5dnd$ (3,j) with j=3/2, 5/2 series members from n=30 to 39. We could not clearly identify members from n =40–45 of this series due to this perturbation. The nature of this broad perturbation is a matter of speculation mainly for two reasons. First, levels based on (a) excited terms of $4f^7$ core (b) excited terms of two-valence electron configurations like $4f^7\,6p^2$ and (c) configurations in which three valence electrons are coupled to a $4f^6$ core are not known in case of europium atom. Even the lower odd parity J=3/2 levels built on configuration $5d\,(^7\boldsymbol{D}_J)\,nl$ are not known. Only three levels of configuration $4f^7\,6p^2\,^{10}\boldsymbol{P}$ term with J=7/2, 9/2, 11/2 are known. Second, the periodicity with respect to the perturbation is not observed in the limited energy region studied in this paper. With these limitations, it was not possible to interpret the perturber at 55 726 cm^{-1} observed in the spectrum by MQDT analysis. Hence we have listed only the observed energy level positions of $5dnd$ (3,j) with j=3/2, 5/2 series members from n=27 to 53 in Table I. Further inputs in the form of identifying lower levels of configurations discussed above and the study of a broader energy region is required to interpret this part of the spectrum.

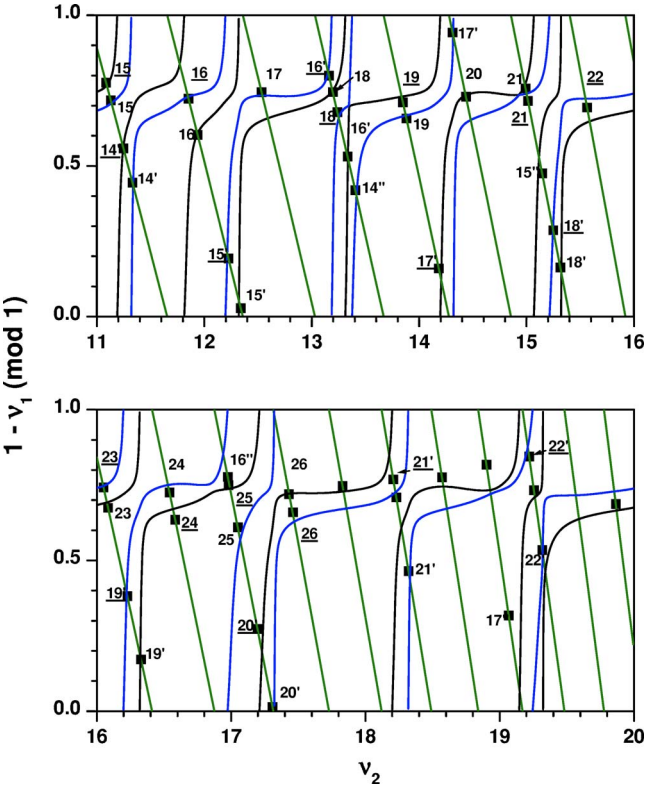

FIG. 3. (Color online) Lu-Fano plot of the J=3/2 autoionization levels converging to the $5d\,^9D$ thresholds. Effective principal quantum numbers ν_1 and ν_2 are calculated with respect to the $5d\,^9D_2$ and $5d\,^9D_3$ ionic limits, respectively. The full curve is calculated with the MQDT parameters listed in Table II. The integers n, $\underline{n}$, n', $\underline{n}'$, and n'' represent principal quantum numbers of levels of configurations $5dnd$ (2,5/2), $5dnd$ (2,3/2), $5dnd$ (3,5/2), $5dnd$ (3,3/2), and $5dnd$ (4,5/2), respectively.

V. CONCLUSION

Multichannel quantum defect theory (MQDT) is applied to interpret perturbations in autoionization Rydberg series in a complex system like europium spectrum. Experimental data from 54 909 to 55 657.74 cm^{-1} are analyzed with a five channel three limit MQDT model. Two-step resonance ionization spectroscopy via the intermediate states $4f^7\,5d6p\,^8P_{5/2,7/2}$ is used for studying odd-parity J=3/2 autoionization Rydberg levels converging to ^9D ionic levels. We have observed two series converging to the $5d\,^9D_2$ limit and another two series converging to the $5d\,^9D_3$ limit. The assignment of the levels is done on the basis of admixture coefficients calculated at the theoretical energies. We have assigned the levels as $5dnd$ (2,j) for the series converging to the $^9D_2$ limit; and the members converging to $^9D_3$ limit are assigned as $5dnd$ (3,j), where j=3/2, 5/2. The two series converging to the lower $^9D_2$ limit are observed experimentally resolved from n=15 to 26 and we could uniquely assign the j value for these levels; whereas from n=27 to 51 the members are unresolved. Similarly, the series converging to the higher $^9D_3$ limit are observed experimentally resolved from n=14 to 24 and unresolved from n=25 to 53. Some of the members these series could not be observed. Five levels

of configuration $5dnd\ (4,5/2)$ are identified in the spectrum. The $5dnd\ (3,j)$ and $5dnd\ (4,5/2)$ are observed to perturb the $5dnd\ (2,j)$ series members. The perturbation analysis is carried out. A relatively broad perturbation observed in the spectrum $\approx$55 726 cm^{-1} has not been interpreted for the reasons discussed. Theoretical energies are calculated and compared with the experimental values. The agreement between theoretical and experimental energies is quite satisfactory.

This work on the analysis of europium spectrum in a limited energy range, above 6*s* continuum and below 5*d* threshold, is very promising in analysis of similar complex spectra. However, the experimental data on higher energy regions and reliable information on identifications of two and three valence electron configurations will allow one to interpret the perturbation mentioned above and will also improve the overall analysis.

ACKNOWLEDGMENT

It is a pleasure to thank Dr. Samuel Cohen of Atomic and Molecular Physics Laboratory, University of Ioannina, Greece for his suggestions and advice in the MQDT work presented in this paper.

[1] M. J. Seaton, Proc. Phys. Soc. London **88**, 801 (1966); Rep. Prog. Phys. **46**, 167 (1983).
[2] K. T. Lu and U. Fano, Phys. Rev. A **2**, 81 (1970); U. Fano, *ibid.* **2**, 353 (1970).
[3] S. Assimopoulos, A. Bolovinos, E. Luc-Koenig, S. Cohen, A. Lyras, P. Tsekeris, and M. Aymar, Eur. Phys. J. D **1**, 243 (1998).
[4] S. Cohen, M. Aymar, A. Bolovinos, M. Kompitsas, E. Luc-Koenig, H. Mereu, and P. Tsekeris, Eur. Phys. J. D **13**, 165 (2001).
[5] M. Aymar, P. Camus, M. Dieulin, and C. Morillon, Phys. Rev. A **18**, 2173 (1978); M. Aymar and O. Robaux, J. Phys. B **13**, 531 (1979).
[6] S. Hasegawa and A. Suzuki, Phys. Rev. A **53**, 3014 (1996).
[7] M. Aymar, A. Debarre, and O. Robaux, J. Phys. B **13**, 1089 (1980); C. B. Xu, X. Y. Xu, W. Huang, M. Xue, and D. Y. Chen, J. Phys. B **27**, 3905 (1994).
[8] G. Smith and F. S. Tomkins, Proc. R. Soc. London, Ser. A **342**, 149 (1975); **387**, 389 (1983).
[9] D. Zyuzikov, V. S. Letokhov, V. I. Mishin, and V. N. Fedoseev, Opt. Spectrosc. **63**, 572 (1987).
[10] S. G. Nakhate, M. A. N. Razvi, G. L. Bhale, and S. A. Ahmad, J. Phys. B **33**, 191 (2000); S. G. Nakhate, M. A. N. Razvi, J. P. Connerade, and S. A. Ahmad, *ibid.* **33**, 5191 (2000).
[11] S. Bhattacharyya, R. D'Souza, Pushpa M. Rao, and M. A. N. Razvi, Spectrochim. Acta, Part B **58**, 469 (2003).
[12] S. G. Nakhate, M. A. N. Razvi, G. L. Bhale, and S. A. Ahmad, J. Phys. B **29**, 1439 (1996).
[13] W. C. Martin, R. Zalubus, and L. Hagan, *Atomic Energy Levels of the Rare Earth Elements*, Natl. Bur. Stand, USA, Circ. 60, 1978.
[14] U. Fano and G. Racah, *Irreducible Tensorial Sets* (Academic, New York, 1959), p. 68.
[15] C. M. Lee and K. T. Lu, Phys. Rev. A **8**, 1241 (1973).
[16] R. D. Cowan, *The Theory of Atomic Structure and Spectra* (University of California Press, Berkeley, 1981).